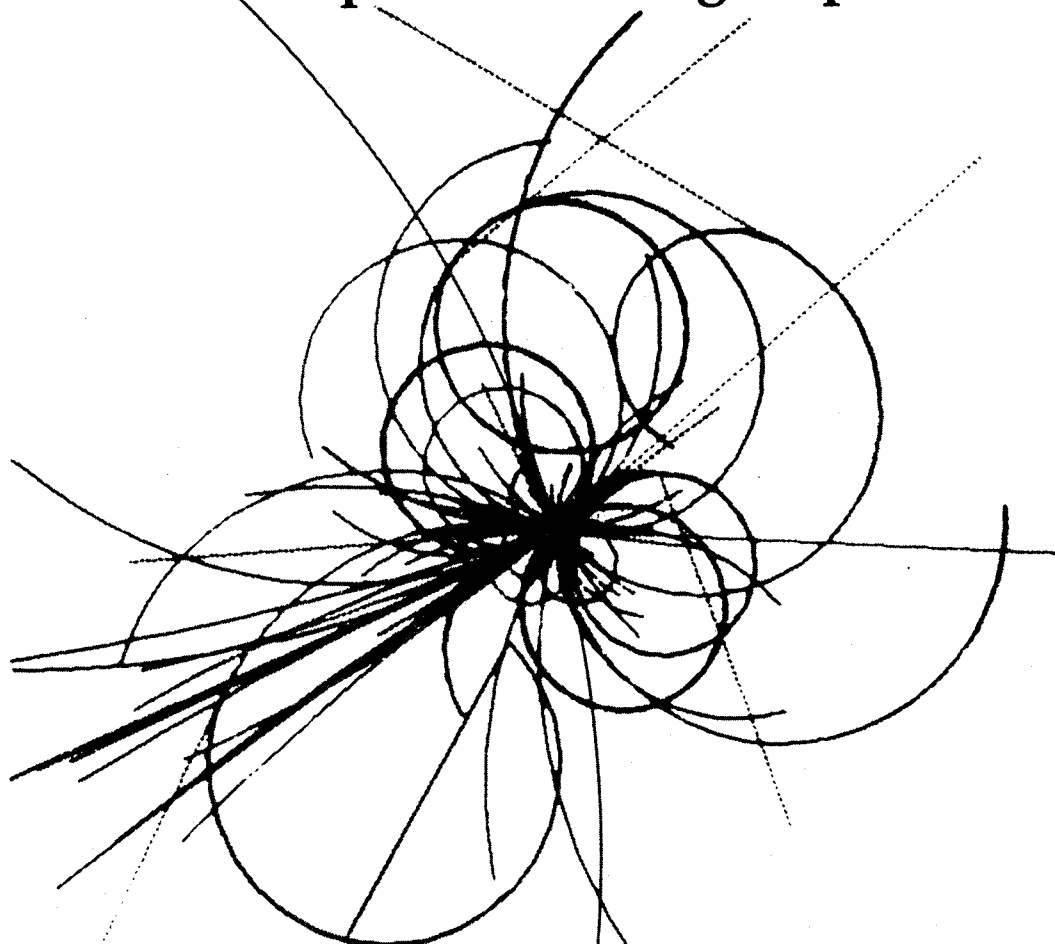


The Superconducting Super Collider



Results of Coherent Dipole Beam-Beam Interaction Studies for SSC Lattices

**Miguel A. Furman
SSC Central Design Group**

May 1986

RESULTS OF COHERENT DIPOLE BEAM-BEAM INTERACTION STUDIES FOR SSC LATTICES

Miguel A. Furman

SSC Central Design Group

May 1986

ABSTRACT

Results are presented for the stability limit of the coherent beam-beam interaction as a function of tune for simplified lattice configurations. The results are obtained from a simulation program in which the beam-beam interaction is represented by one-dimensional linear kicks, and the bunches are considered to be rigid charged objects (dipole approximation). For nominal SSC parameters we find that the coherent beam-beam interaction introduces serious instabilities only in very narrow regions of tune around integers or half-integers (depending on the symmetry of the lattice considered), and therefore does not restrict the choice of tune significantly.

INTRODUCTION

The fact that the SSC has many thousands of closely spaced bunches suggests that the beam-beam interaction may have an important effect on beam stability. Indeed, with a nominal interbunch distance of 4.8 m and interaction regions (IRs) of up to 300 m in length, the number of bunches simultaneously within an IR reaches 63. Thus a given bunch collides up to 126 times with the oncoming bunches before leaving the IR. Of course only one of these collisions is desirable: it is the head-on collision at the center of the IR which will yield the new discoveries in particle physics for which the SSC is planned. The other "collisions" on either side of the center of the IR are long-range and purely electromagnetic in character, and are unavoidable because of the small crossing angle of the beams. Both types of collisions have a potential detrimental effect on beam stability, which is quickly compounded as the bunches circulate many times around the machine. We are compelled, therefore, to assess the importance of the beam-beam interaction.

In previous notes [1,2] we presented preliminary results for this problem for simplified lattice geometries with identical IRs, identical arcs and up to 36 bunches per beam. The present note extends those results to more realistic lattices in which the IRs are not identical, the arcs have different lengths (clustered IRs), and the beams have gaps ("pac-man" effect). The largest number of bunches we consider here is 332 per beam which is much less than the nominal 17,280 of the SSC. However, we have found that the results for stability limits are quite insensitive to the number of bunches in the arcs, and are sensitive only to the number of bunches in the IRs. Thus our final conclusions are based on simulations in which the IRs have the realistic lengths (300 m and 144 m, corresponding to 63 and 29 bunches respectively) but the arcs are much shorter than their nominal length.

Our main conclusion is that the coherent beam-beam effect poses no significant stability problems for the SSC. Only very narrow bands of instability appear around integer or half-integer tune; since these values are to be avoided anyway, our results imply no significant constraint on the tune choice. The reason for this result is that, although the beam-beam collisions are many, their individual strength is small on account of the low number of particles per bunch.

ANALYSIS

Interaction Regions

Consider one bunch from either of the oncoming beams within an IR before they have had time to be separated into their respective beam pipes. The bunches are at a distance x_1 and x_2 from their respective design trajectories, which are separated by a distance d , as shown in Fig. 1. We shall consider motion in one transverse dimension only, so that the design trajectories and the bunch motion are contained in one plane. The actual distance between the bunches is $r = d + \Delta x$ where $\Delta x = x_1 - x_2$. Although the form of the charge distribution is irrelevant for the dipole motion, we consider a Gaussian shape for the purpose of this discussion. Since the bunches are short and relativistic, the impulse approximation for the force is valid, so the kick the bunches experience is described by the change in slope

$$\Delta x_1' = -\Delta x_2' = (1/f) [E(d + \Delta x, \sigma) - E(d, \sigma)] \quad (1)$$

where f is the effective focal length of the force, σ is the transverse rms bunch size and E is the

function

$$E(x, \sigma) = (2\sigma^2/x) [1 - \exp(-x^2/2\sigma^2)] \quad (2)$$

which is depicted in Fig. 2. In Eq. (1) we have subtracted the $E(d, \sigma)$ -term corresponding to a background force induced by the design trajectory, which we assume is compensated for by some appropriate mechanism which does not concern us (this term vanishes for the head-on collision, where $d=0$). The strength $1/f$ of the kick is given by

$$1/f = 4\pi\xi/\beta \quad (3)$$

with

$$\xi \equiv N_B r_o / (4\pi \epsilon_N)$$

where β is the beta-function at the collision point, ϵ_N is the normalized emittance, N_B is the number of particles per bunch and r_o is the classical radius of the particle.

We assume that the bunches simply drift between successive collisions within a given IR. Therefore, for a collision that takes place at a distance s from the center of the IR, $\beta(s)$, $\sigma(s)$, and $d(s)$ are given by

$$\begin{aligned} \beta(s) &= \beta^* (1 + s^2/\beta^{*2}) \\ \sigma(s) &= \sqrt{\epsilon \beta(s)} \\ d(s) &= \alpha s \end{aligned} \quad (4)$$

where α is the (full) crossing angle, β^* is the beta-function at the center of the IR and ϵ is the emittance, $\epsilon = \epsilon_N/\gamma$, γ being the usual relativistic factor. Of course ξ is independent of s .

For the head-on collisions the bunches overlap significantly, so it is legitimate to expand (2) around $x=0$, where the force is approximately linear; thus we get

$$\Delta x_1' = -\Delta x_2' = (4\pi\xi/\beta^*) \Delta x \quad (\text{head-on}) \quad (5)$$

Since the bunch separation is $S_B = 4.8$ m, the strongest long-range collision (the one closest to the center of the IR) occurs at a distance $d_1 = \alpha S_B/2 = 180 \mu\text{m}$ (we use the nominal value $\alpha = 75 \mu\text{rad}$). If we compare the typical beam size $\sigma(s)$ with the typical separation $d(s)$ for any of the long range collisions, we obtain ratios $\sigma(s)/d(s) \leq 0.13$ for the high-luminosity IRs ($\beta^* = 0.5$ m) and even smaller ratios for the medium-luminosity IRs ($\beta^* = 10$ m). Thus it is legitimate to expand (2) out in the $1/x$ tail, and we get

$$\Delta x_1' = -\Delta x_2' = -(4\pi\xi/\beta^*) P(s) \Delta x \quad (\text{long-range}) \quad (6)$$

where

$$P(s) \equiv 2(\sigma^*/d(s))^2 = 2 \epsilon \beta^* / (\alpha s)^2 \quad (7)$$

is a dimensionless parameter that characterizes the strength of the long-range vs. head-on collisions, and $\sigma^* \equiv \sigma(0)$. The negative sign in (6) arises from the negative slope of (2) at large distance. Since we are only considering *deviations* from the design trajectory, this negative sign only means that the long-range kicks get relatively weaker as the bunches get further away from the design trajectory, as is clear from Fig. 2. The net force is indeed repulsive for all kicks for like-sign beams.

In order to get an idea of this relative strength, we consider again the strongest long-range collision where $s = S_B/2 = 2.4$ m. For the nominal SSC parameters $\epsilon_N = 10^{-6}$ m-rad and $\gamma = 21,322$ we obtain $\epsilon = 4.7 \times 10^{-11}$ m-rad so that $P(S_B/2) = 2.9 \times 10^{-2}$ for $\beta^* = 10$ m and 1.45×10^{-3} for $\beta^* = 0.5$ m. While these numbers are small, the cumulative effect over the length of the IR is significant. To see this, we calculate from Eqs. (5) and (6) the lowest-order tune shift per IR, and we get, for an IR of half-length L ,

$$\begin{aligned} \Delta \nu_{HO} &= -\xi \\ \Delta \nu_{LR} &= 8 \xi (L/S_B) (\sigma^*/(\alpha \beta^*))^2 \end{aligned} \quad (8)$$

For a medium-luminosity IR ($L=150$ m, $\beta^*=10$ m) we obtain $\Delta \nu_{LR} \approx 0.2 \xi$, while for a high-luminosity IR ($L=72$ m, $\beta^*=0.5$ m), $\Delta \nu_{LR} \approx 2 \xi$. Thus the long-range collisions are important relative to the head-on. However, from Eq. (3), using the nominal value for ϵ_N given above and $N_B = 7.3 \times 10^9$, and $r_0 = 1.535 \times 10^{-18}$ m, we get $\xi = 0.9 \times 10^{-3}$ which is small. In our simulation we will obtain the maximum value of ξ for which there is stable motion for each value of the tune, and we will later compare this stability boundary with the above nominal value of ξ .

Arcs

Consider a bunch moving from IR no. 1 to IR no. 2., as in Fig. 3. The corresponding phase advance matrix between the centers of the IRs is

$$T_{21}^* = \begin{bmatrix} \sqrt{\beta_2^*/\beta_1^*} C & \sqrt{\beta_2^* \beta_1^*} S \\ -\frac{S}{\sqrt{\beta_2^* \beta_1^*}} & \sqrt{\beta_1^*/\beta_2^*} C \end{bmatrix} \quad (9)$$

where $S = \sin(2\pi v^*)$, $C = \cos(2\pi v^*)$ and v^* is the tune from the center of IR1 to the center of IR2. In practice, however, we need the matrix T_{21} from the exit of IR1 to the entrance of IR2; if L_1 and L_2 are the half-lengths of the IRs, it is given by

$$T_{21}^* = D(L_2) T_{21} D(L_1) \quad (10)$$

or

$$T_{21} = D(-L_2) T_{21}^* D(-L_1) \quad (11)$$

where $D(L)$ is a drift matrix for a distance L ,

$$D(L) = \begin{bmatrix} 1 & L \\ 0 & 1 \end{bmatrix} \quad (12)$$

Simulation method

The ingredients for the simulation are now completely described: a bunch, represented by its transverse coordinates (x, x') is either kicked by an opposing bunch according to Eqs. (5) or (6), or drifted between successive collisions by a matrix $D(S_B/2)$, or transported from the end of an IR to the beginning of the next one by the appropriate matrix T_{21} given by Eq. (11). In order to complete the description of the simulation we need to specify a lattice configuration, an initial beam configuration, and a stability criterion.

The lattice configuration is described by (a): the number of IRs, their lengths (in units of S_B) and their β^* , and (b): the number of arcs (equal to the number of IRs), their lengths (also in units of S_B) and their tune v_i^* . Some of the arcs may have a fixed tune specified a priori; if this is the case, the tune of the remaining arcs is calculated by subtracting the sum of the fixed tunes from the tune of the whole ring v and dividing this equally among the arcs with variable tune. If there are no fixed-tune arcs, their tune is equal to the tune of the whole ring divided by the number of arcs. In either case the tune is taken to be independent of the arc length.

The initial beam configuration is specified by assigning initial values to (x, x') for all bunches of both beams. The number of bunches per beam is obviously determined by the lattice configuration just described, except that there may be gaps in the bunch population of either or both beams. If this is the case, the number and length of the gaps is recorded by the program. The initial values for x and x' are taken to be random numbers distributed uniformly in the ranges $(-x_0, x_0)$ and $(-x_0', x_0')$ respectively. The values for x_0 and x_0' are chosen to be equal to 1/10th of the smallest of the roughly estimated typical values found around the ring, namely $x_0 = 0.5 \mu\text{m}$ and $x_0' = 0.05 \mu\text{rad}$ respectively [3].

Finally, the stability criterion we adopt is as follows: after each "step", which is defined below, if any of the values of $(x/\sqrt{\beta^*})$, measured at the center of the IRs, exceeds $2\sqrt{\epsilon}$, we call the motion unstable; if no instability is found after a certain number of turns, we call the motion stable (a further discussion is given below).

Having specified the lattice and beam configurations, we assign a value to the tune of the whole ring ν , and the parameter ξ , and run the program to determine whether the motion is stable or not. By changing these we find the stability boundary in the (ξ, ν) -plane.

The program keeps track at all stages of the values of (x, x') for all bunches of both beams, as well as their location around the ring. As mentioned above, the bunches are either kicked, drifted or transported. This is done for all bunches, and this constitutes one "step". Physically, one step corresponds to the whole beam moving by a distance $S_B/2$. The maximum number of turns allowed depends on the number of bunches. For small numbers (up to 36), we have found that 50 turns is, in most cases, more than adequate. For larger numbers of bunches, we use up to 1000 turns, although in most cases fewer turns suffice. The stability criterion described above, including the appropriate number of turns, has been arrived at by successive experimentation. In most cases, unstable motion manifests itself very quickly and clearly, and therefore is easy to detect. In a few exceptional cases, barely unstable motion takes a long time to exceed the stability criterion, so we have to increase the maximum allowed number of turns. Stable motion is, of course, harder to establish because of the lack of a positive signal. In most cases, however, stability is fairly obvious because the values of x at the center of the IRs are fairly constant or oscillate gently around some mean value. In a very few doubtful cases we successively increased the maximum allowed number of turns by factors of 2. The stability criterion is such that our results agree with high accuracy with analytic results whenever available [4], or with matrix eigenvalue calculations we have performed as a check in a few simple cases.

RESULTS

In all figures we show the stability limit of the parameter ξ vs. the tune ν of the whole ring, and plot only one period of the curve. We define here m and m' to be:

$$\begin{aligned} m &= \text{number of bunches in an IR} \\ m' &= \text{number of bunches in an arc} \end{aligned}$$

Identical distributed IRs

For completeness, we present first some results for simple lattice configurations with identical IRs and identical arcs evenly distributed around the ring.

Fig. 4 shows the results for a lattice with 2 IRs with $\beta^* = 1$ m, $\sigma^* = 7$ μ m (corresponding to an emittance $\epsilon = 4.9 \times 10^{-11}$ m-rad), and $m = 2$, $m' = 0$ (total of 4 bunches per beam). The 3 curves correspond to 3 values of the crossing angle: for $\alpha = 50$ μ rad the stability curve is ACE; for $\alpha = 10$ μ rad it is ABE, and for $\alpha = 1$ rad it is ABCD. As the crossing angle is increased, the long-range collision strength decreases as α^{-2} , according to Eq. (7), so the stability region correspondingly grows. The positive-slope branches of the curves (AB, AC) are essentially determined by the head-on collisions, while the negative-slope branches (BE, CE) by the long-range collisions; this is a general feature of all our results. The curve with $\alpha = 1$ rad has little physical meaning, but it is a useful limiting case in which the long-range collisions are negligibly small. In this case, the curve is identical to the one obtained with 1 bunch per IR and an arbitrary number of bunches in the arcs

(including zero), and whose analytic expression [5] is given by $\xi = \tan(\pi\nu/2)/(4\pi)$.

Fig. 5 shows the result for a lattice with 4 IRs with $\beta^* = 1$ m and $m = 1$, $m' = 0$ (i.e., only head-on collisions). It agrees with the analytic result [4] $\xi = (1-C)/(4\pi S)$, and $\xi = -C/(4\pi S)$ for the 2 branches, respectively, where $S \equiv \sin(\pi\nu/2)$ and $C \equiv \cos(\pi\nu/2)$.

Fig. 6 shows the results for a lattice with 6 IRs with $\beta^* = 1$ m, $\sigma^* = 7$ μ m and $m = m' = 3$ (36 bunches per beam). As in Fig. 4, the 3 curves correspond to 3 different crossing angles: for $\alpha = 50$ μ rad the stability curve is ACA'C'A"C"E; for $\alpha = 10$ μ rad it is ADA'D'A"D"E, and for $\alpha = 1$ rad it is ABA'B'A"B". This latter one is, again, the limiting case in which the long-range collisions are negligibly small, and the curve is identical to the one obtained with 1 bunch per IR and an arbitrary number of bunches in the arcs (including zero), and whose analytic [4] expression is given by $\xi = (1-C)/(4\pi S)$, $\xi = (1/2-C)/(4\pi S)$, and $\xi = -(1/2+C)/(4\pi S)$ for the 3 branches, respectively. Here $S \equiv \sin(\pi\nu/3)$ and $C \equiv \cos(\pi\nu/3)$. Clearly a nominal value of $\xi = 0.9 \times 10^{-3}$ would imply only tiny regions of instability around integer values of tune.

Fig. 7 shows a comparison of different beam configurations for a lattice with 6 IRs and $\beta^* = 1$ m, $\sigma^* = 7$ μ m, and crossing angle $\alpha = 50$ μ rad. The 3 curves correspond to $(m, m') = (3, 3)$, $(5, 1)$, and $(13, 20)$ which have, therefore, 36, 36, and 198 bunches per beam, respectively. The $(3, 3)$ case is ABA'B'A"B"E, already shown in Fig. 6. The $(5, 1)$ case is ACA'C'A"C"E, and the $(13, 20)$ is ADA'D'A"D"E. Note that the larger m is the stronger is the long-range instability, as evidenced by the negative slope branches, which are closer to the horizontal. We have also obtained the stability curves for $(m, m') = (3, 10)$ and $(5, 100)$, but these are not plotted because they are identical, at least within our accuracy, to the cases $(3, 3)$ and $(5, 1)$ respectively. Clearly there is a much greater sensitivity to m than m' .

Beam gaps

Fig. 8 also corresponds to a lattice with 6 IRs with $\beta^* = 1$ m, $\sigma^* = 7$ μ m, $\alpha = 50$ μ rad and $(m, m') = (13, 20)$ (total of 198 bunches per beam). The solid line corresponds to the no-gap case, already shown in Fig. 7. The dashed line corresponds to the case in which there is one gap of 13 missing bunches in each beam. The beam configuration in which the simulation is initially launched is such that the two gaps are about to "collide" at the center of one of the IRs (whenever the dashed line is not shown it coincides with the solid line within our accuracy). We have also obtained results for a few other gap configurations, e.g., when only one of the beams has a gap, and when there are up to 6 gaps per beam. All these results are quite similar to the ones shown, so they are not exhibited for clarity. We point out, however, that as the total gap size becomes substantial, i.e., about half of the total number of bunches, the stable region becomes larger and larger, as it seems clear it should.

Identical clustered IRs

Fig. 9 shows a comparison of results between distributed and clustered IRs. All 3 curves correspond to 6 identical IRs with $\beta^* = 1$ m, $\sigma^* = 7$ μ m, $\alpha = 50$ μ rad and $m = 13$, but with different arcs. The clustering scheme is the so-called $(3, 3)$, in which there are 2 long arcs and 4 short arcs [2]. The solid line corresponds to the distributed IR case with $m' = 20$, already shown in Fig. 7. For the dashed line case, the short arcs and the long arcs have $m' = 1$ and 10, respectively

(total of 102 bunches per beam), while the dotted line corresponds to $m'=5$ and 50 (198 bunches per beam). Wherever the curves overlap, only the solid line is shown. All arcs have the same tune. Again we observe little sensitivity to the length of the arcs. The results of a few other beam configurations, which are not shown here, tend to support this conclusion.

Fig. 10 shows the results for the same clustered IRs of Fig. 9, except that the tune of the short arcs is held fixed at 0.25. The long arcs have equal, variable tune so that the tune of the whole ring is what is shown. The solid line corresponds to $m'=1$ and 10, and the dashed line to $m'=5$ and 50 for the short and long arcs, respectively. The curves overlap except in the middle section.

Fig. 11 shows results for the same 6 IRs as in the previous case, except that they are clustered according to the (4,2)-scheme. Again the tune of the short arcs is held fixed at 0.25, but only one beam configuration is presented, namely $m=13$, $m'=1,10$. Note the additional zeroes of the stability curve at half integers appearing because the mirror symmetry of the ring has been broken, that is, any pair of bunches from either beam collide only once around the ring rather than twice, as in all previous examples.

Nominal CDR lattices

Fig. 12 shows the stability limit results for a lattice with 4 IRs of two kinds. The lattice is described as follows: two high-luminosity IRs ($\beta^* = 0.5$ m) are clustered together, and two medium-luminosity IRs ($\beta^* = 10$ m) are clustered together diametrically opposite to the previous ones. The emittance is a nominal $\epsilon = 4.69 \times 10^{-11}$ m-rad, which translates into $\sigma^* = 4.5$ μ m for the low- β IRs and $\sigma^* = 21.7$ μ m for the high- β IRs. The crossing angle is a nominal $\alpha = 75$ μ rad. All 4 IRs have $m=1$ bunch. The short arcs between the two IRs within each cluster have $m'=1$ bunch, and the long arcs between the clusters have $m'=10$ bunches (total of 26 per beam). The short arc between the two low- β IRs has a fixed tune of 3.75, and the short arc between the two high- β IRs has a fixed tune of 3.25. The long arcs have equal, variable tune. Since $m=1$ for all IRs, there are only head-on collisions. The novel boat sail shape is due to the inequality between the IRs. This curve should be contrasted with the symmetric case of Fig. 5.

Fig. 13 corresponds to the same lattice as in Fig. 12, except that here long-range collisions are included. The IRs have their nominal lengths, so that the low- β IRs have $m=29$ bunches while the high- β IRs have $m=63$ bunches (206 bunches per beam). The 3 curves correspond to the cases in which the crossings are purely "vertical", purely "horizontal", or they "alternate" between the two from IR to IR. The parameter ξ is the vertical head-on tune shift; the stability diagram for the horizontal tune shift is obtained by reversing the solid and dashed curves. Since our program is for one-dimensional simulations only, by "vertical" kicks in a vertical-crossing IR we mean that the long-range kicks have the usual minus sign, as in Eq. (6), and by "horizontal" we mean that they have a plus sign [6].

Finally, Fig. 14 shows the results for a nominal lattice with 6 IRs (which includes the "future" IRs in addition to the 4 discussed in the previous case). The lattice has 2 clusters: one with 2 low- β IRs with $m=29$ bunches each, and another one with 4 high- β IRs with $m=63$ bunches each. The low- β IRs are separated by a short arc with $m'=1$ and fixed tune of 3.75. The high- β IRs are separated by short arcs with $m'=1$ and fixed tune of 3.25. The 2 clusters are not diametrically opposed, so they are separated by arcs of unequal length of $m'=8$ and $m'=10$ for a total of 332

bunches per beam. The tune of the long arcs are variable and equal. Only vertical crossings are considered.

CONCLUSIONS

It is apparent from the stability diagrams presented, especially for the nominal cases presented in Figs. 12 through 14, that the coherent beam-beam force implies no restriction on the tune choice for a nominal $\xi = 0.9 \times 10^{-3}$ except very near integer or half-integer tunes, which are to be avoided anyway. Gaps in the bunch population of the beams and clustering of the IRs do not have a qualitative effect on the stability. Although our simulation describes the dipole approximation only, our conclusions remain valid when higher-order multipoles are included, at least for symmetrical lattices and beams with no gaps [7].

Of course it would be desirable to extend our simulation to more realistic cases, but this does not seem justified at this stage. Besides, the program used here is already very time-consuming: the CPU time per turn is approximately given by

$$T = K \cdot M_{IR} \cdot M \quad (13)$$

where M_{IR} is the total number of bunches in all the IRs, M is the total number of bunches per beam and K is a computer-dependent constant with units of time which, for Livermore's Cray-XMP (on which all our runs have been made) is approximately 8×10^{-5} sec (we have made no serious attempt to optimize our program for the Cray's hardware). When we consider that for every value of tune about 300 to 500 turns are required (for large number of bunches) in order to find the stability point with reasonable accuracy, and that a minimum of 20 to 50 values of tune are required for a sensible boundary curve, we can easily run into CPU times of 50 to 100 hours, and therefore a different method is required.

ACKNOWLEDGMENTS

I am pleased to thank Alex Chao for his continuing interest in this problem and to Etienne Forest for many useful discussions.

REFERENCES AND FOOTNOTES

- [1] M. A. Furman and A. W. Chao SSC-28 (1985), proc. 1985 Particle Accelerator Conf. (Vancouver), IEEE Trans. Nucl. Sci., vol. NS-32, No. 5 (1985), p.2297 and references therein.
- [2] The Clustered Interaction Region Option for the SSC, report no. SSC-SR-1014.
- [3] For the low- β IRs the typical amplitude and slope are $x_{IR} \approx \sigma^* \approx 5 \mu\text{m}$ and $x'_{IR} \approx \sigma^* / \beta^* \approx 10 \mu\text{rad}$. In the arcs, the typical values are $x_{ARC} \approx \sqrt{\epsilon \beta_{ave}} \approx 88 \mu\text{m}$ and $x'_{ARC} \approx \sqrt{\epsilon / \beta_{ave}} \approx 0.5 \mu\text{rad}$, where we use $\beta_{ave} = 170 \text{ m}$. Thus the lowest estimated values for x and x' around the ring are $5 \mu\text{m}$ and $0.5 \mu\text{rad}$ respectively. We use 1/10th of these numbers as a starting point in our simulation.

- [4] E. Forest and M. Furman, SSC-32 (1985).
- [5] A. Piwinski, Proc. VIII Int. Conf. High Energy Accel., CERN, p.357 (1971); A.Chao and E. Keil, CERN/ISR-TH/79-31 (1979); A. Chao, AIP Proc. no. 57, 1979.
- [6] S. Heifets, private comm.; A. Chao and S. Peggs, SSC-N-80; S. Peggs, SSC-63 (1985)
- [7] E. Forest, SSC-51

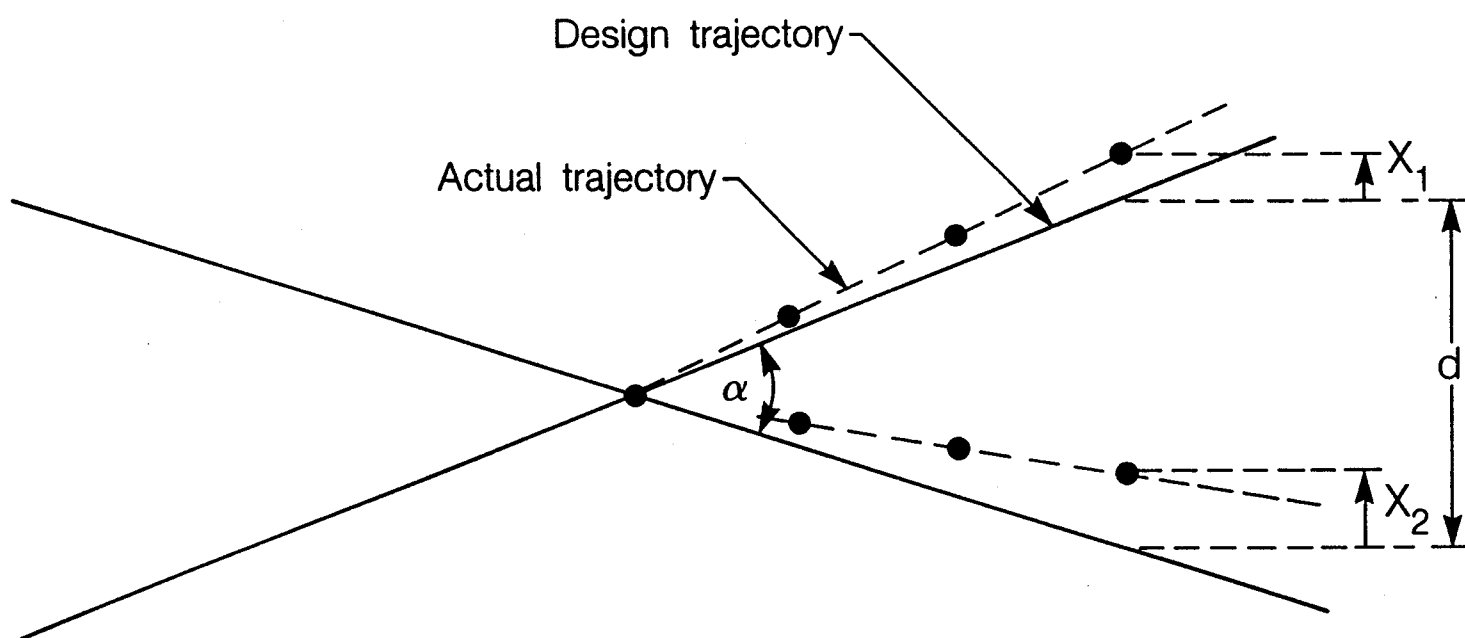


Fig. 1 Three long-range collisions and one head-on collision in an IR.

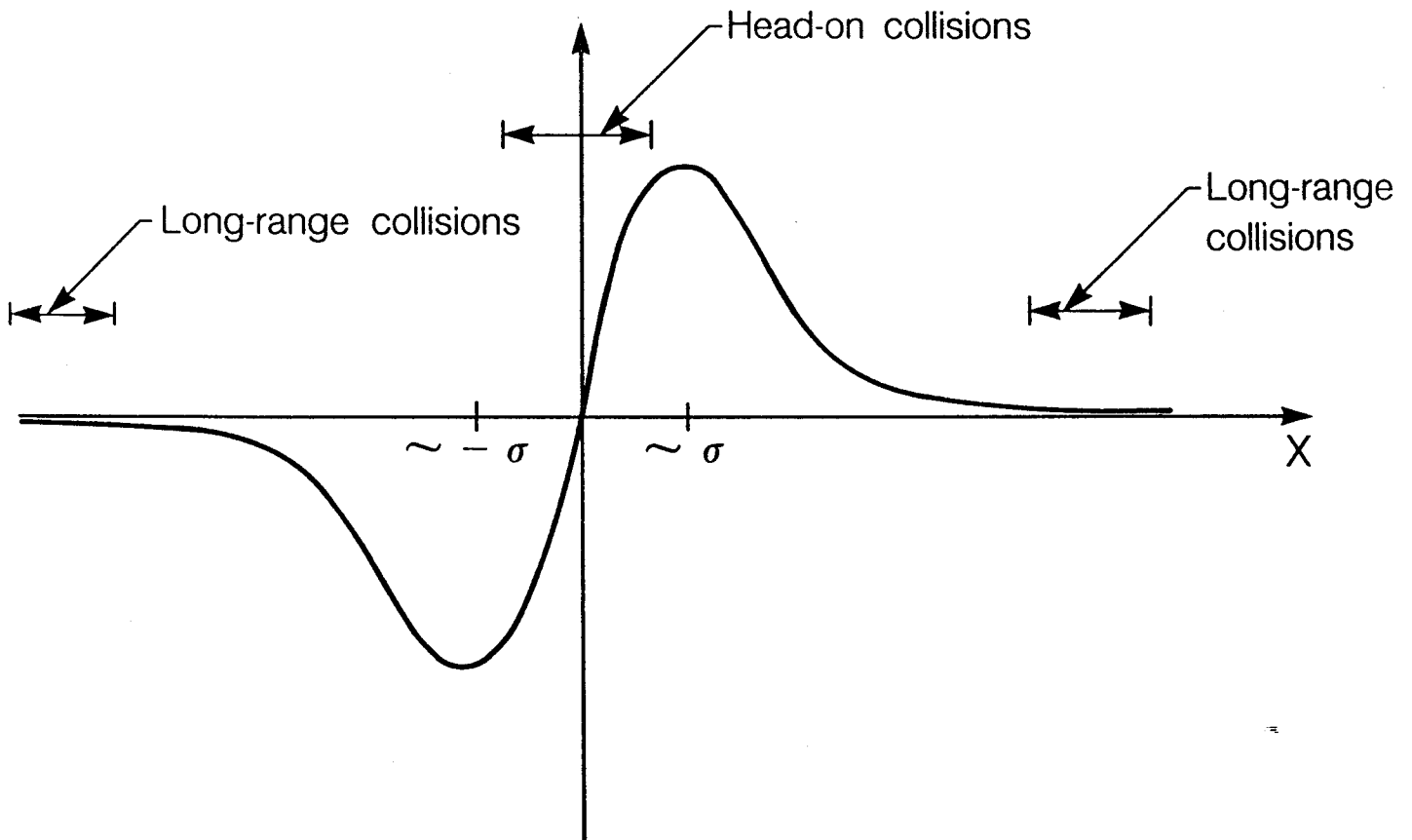


Fig. 2 Beam-beam force vs. bunch separation, showing the typical regions sampled by the head-on and long-range collisions.

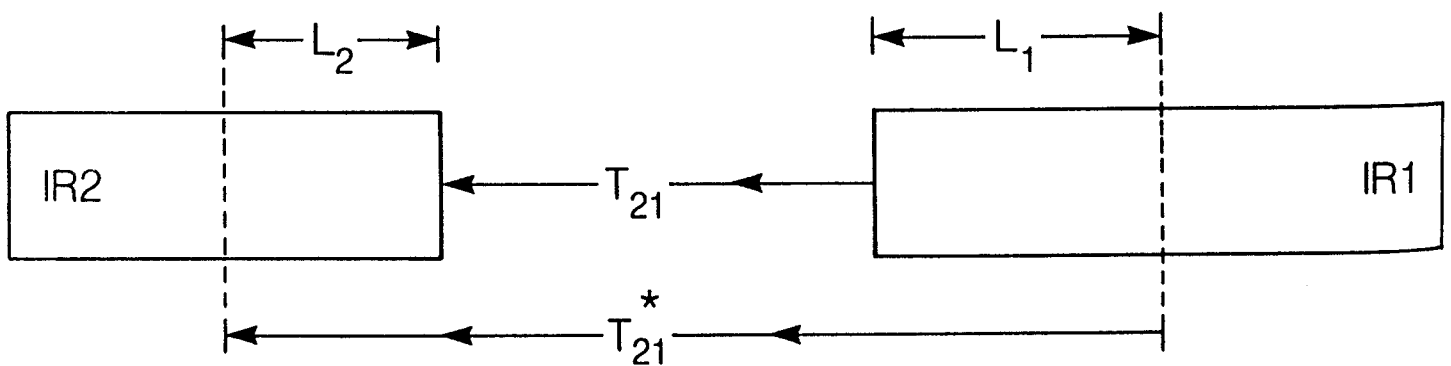


Fig. 3 Transport matrix between two IRs of different lengths (see Eq. (10)).

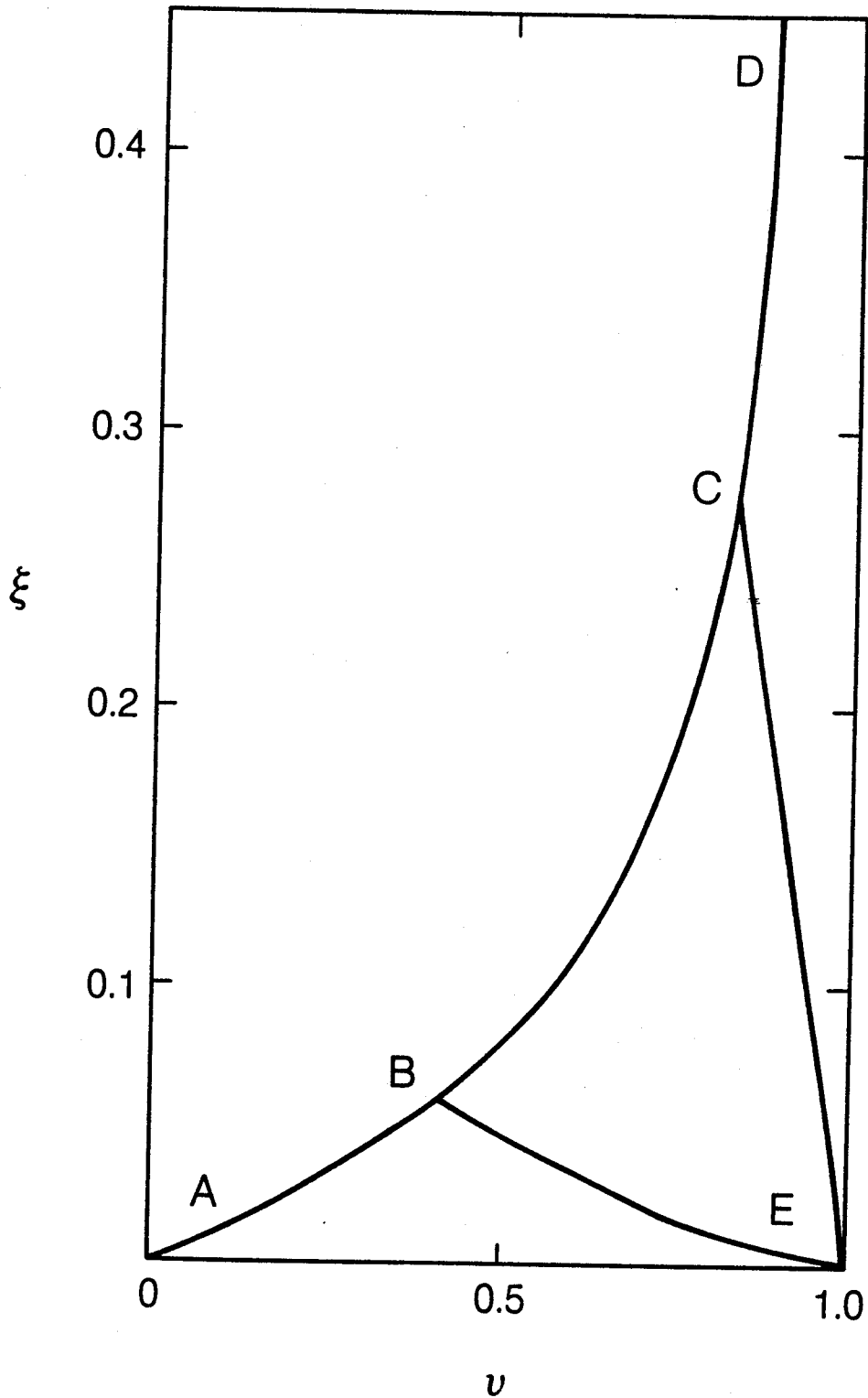


Fig. 4 Stability diagram for a lattice with two identical distributed IRs and 4 bunches per beam. The regions above the curves are unstable. Curve ABE corresponds to a crossing angle of $10 \mu\text{rad}$, ACE to $50 \mu\text{rad}$, and ABCD to 1 rad .

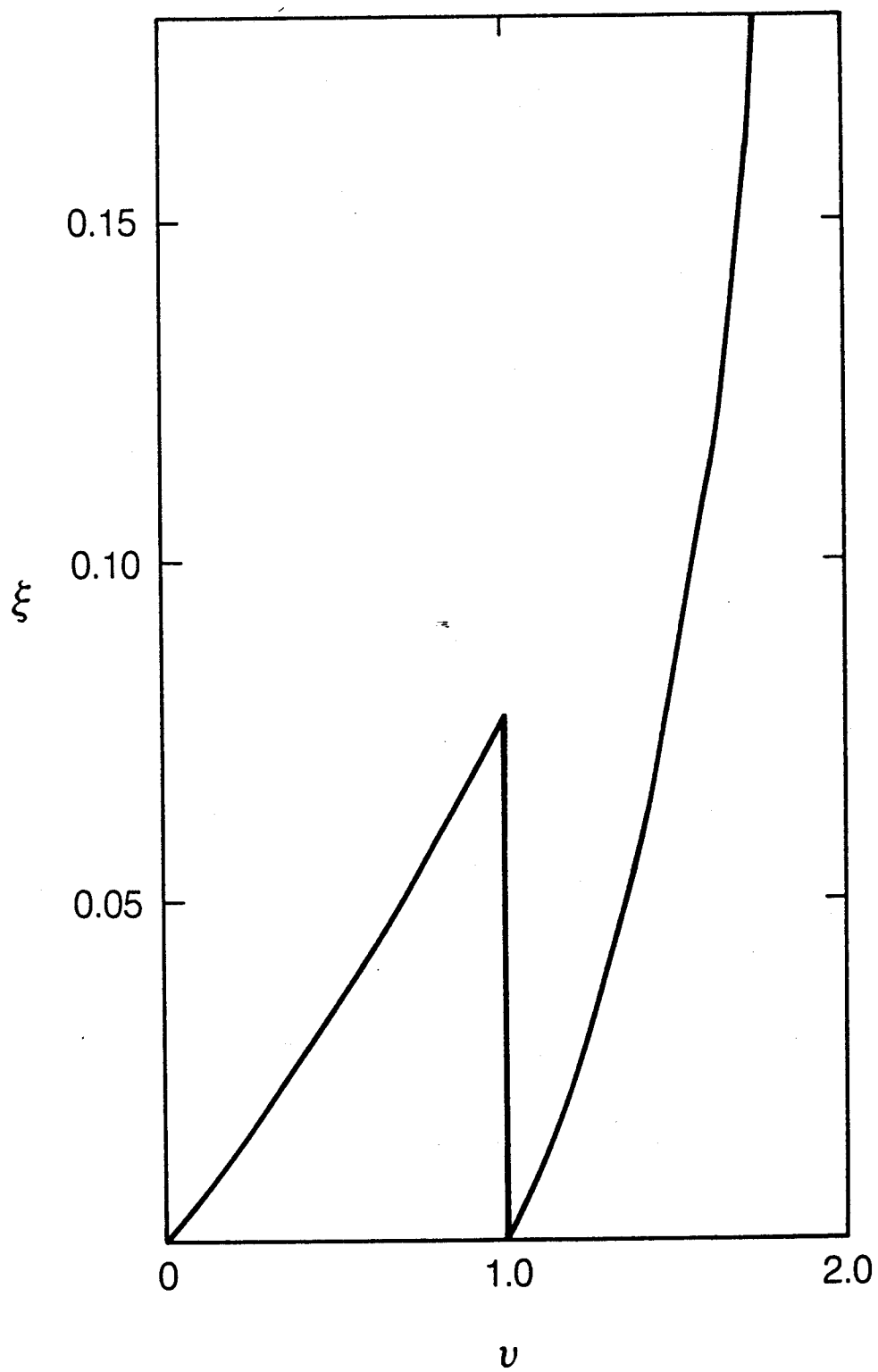


Fig. 5 Stability diagram for four identical distributed IRs and 4 bunches per beam.

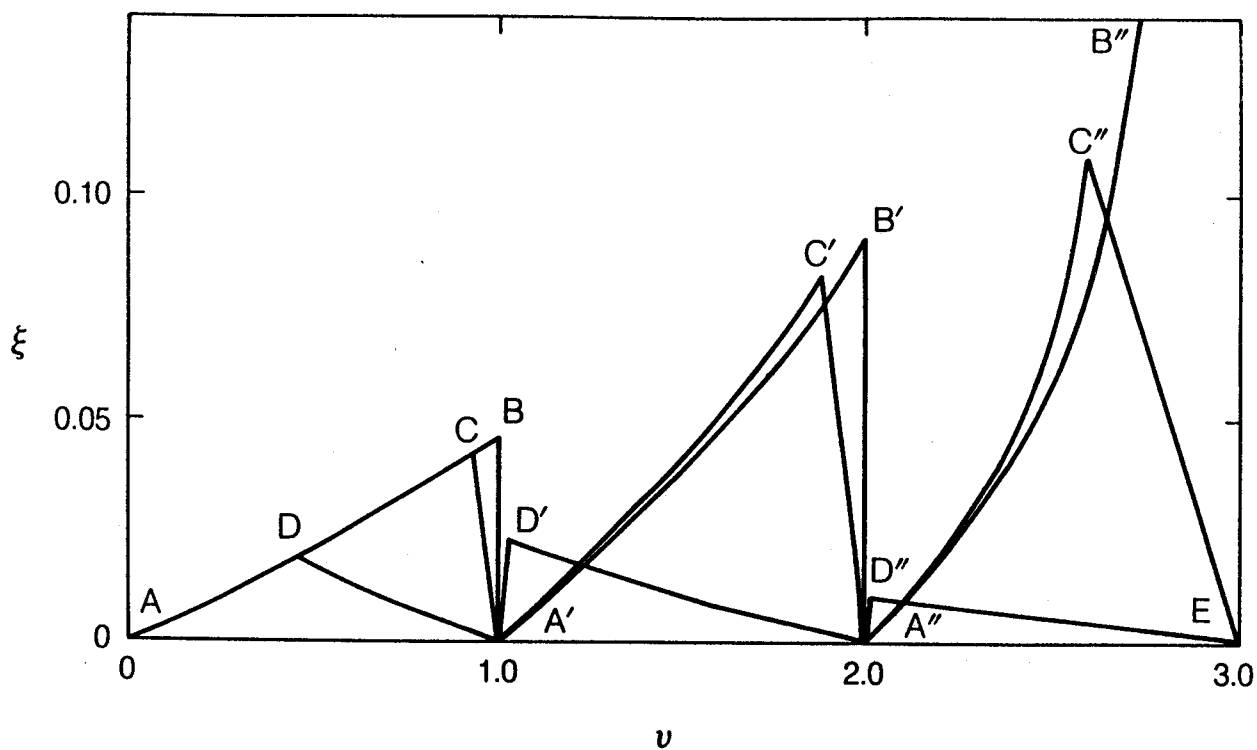


Fig. 6 Stability diagram for six identical distributed IRs and 36 bunches per beam. ADA'D'A''D''E corresponds to a crossing angle of 10 μ rad, ACA'C'A''C''E to 50 μ rad, and ABA'B'A''B'' to 1 rad.

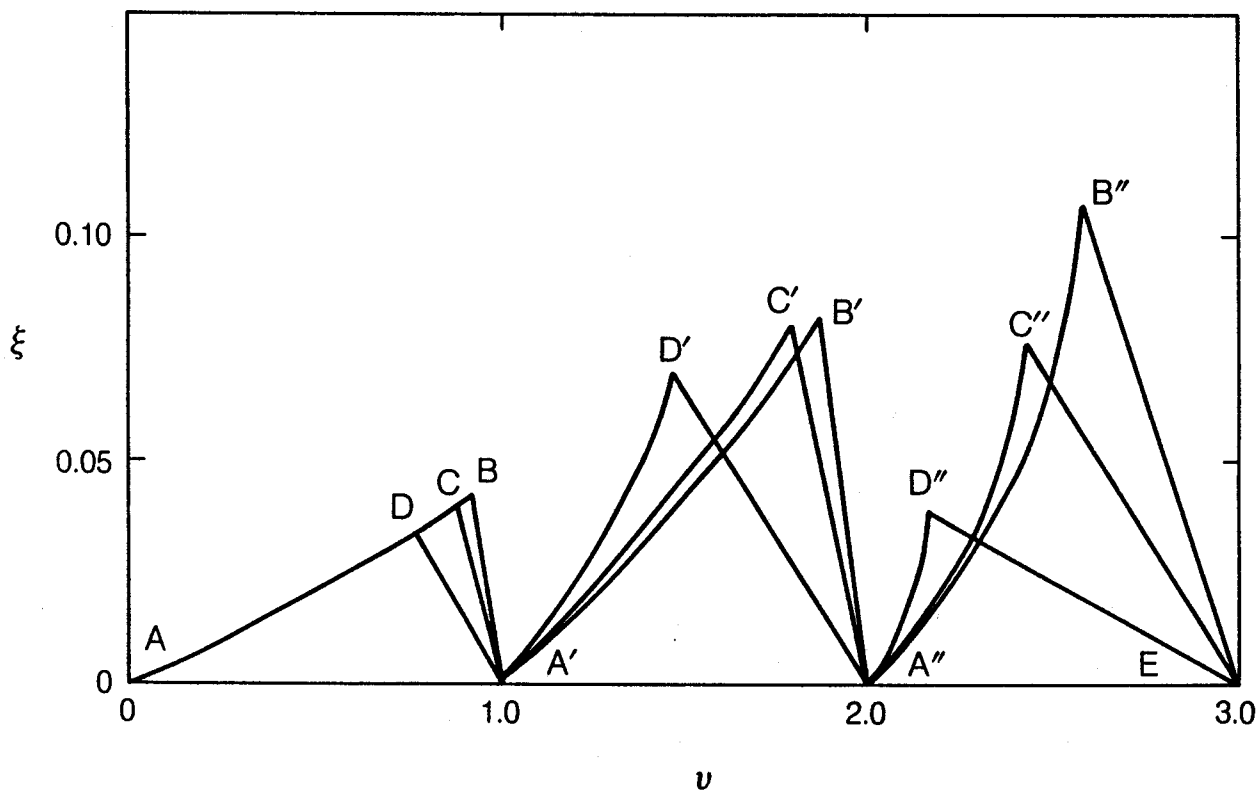


Fig. 7 Stability diagram for six identical distributed IRs. The 3 curves correspond to different beam configurations, with different numbers of bunches per IR and per beam. See text for a detailed explanation.

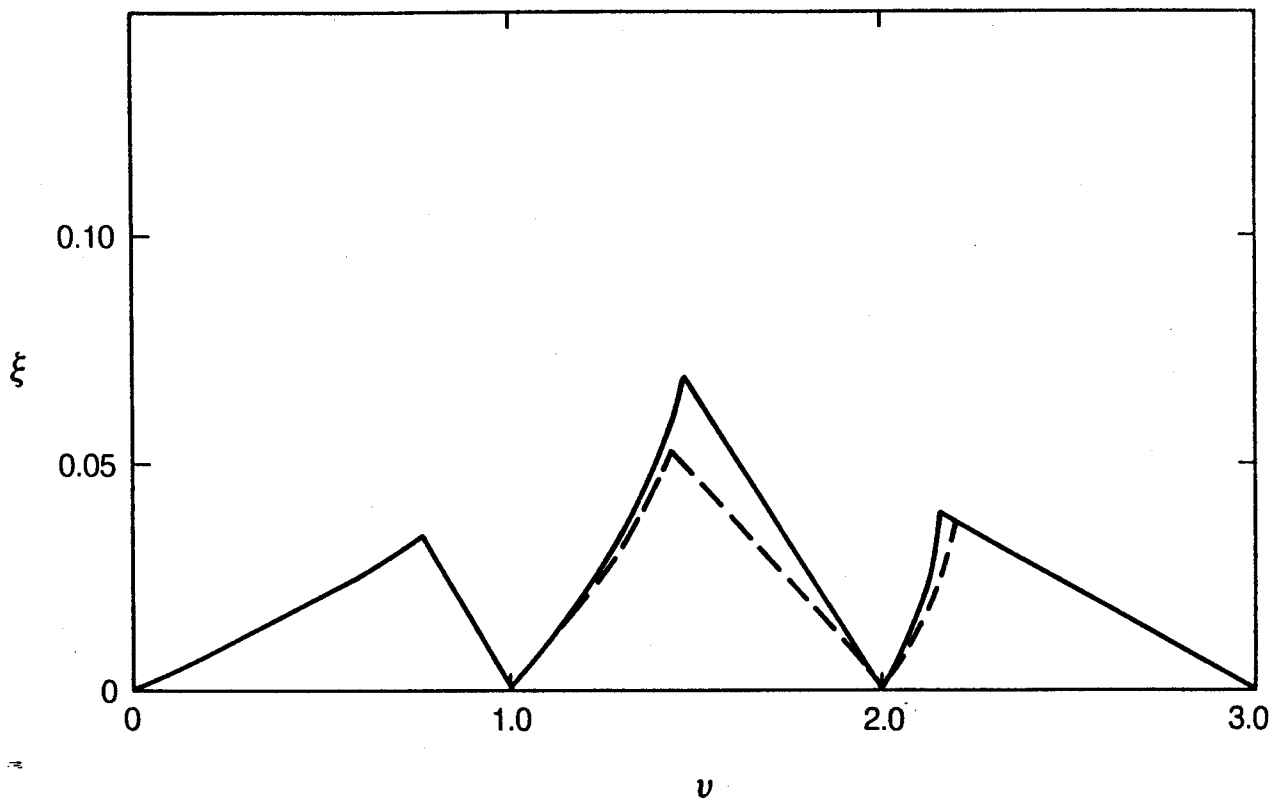


Fig. 8 Stability diagram for six identical distributed IRs and 198 bunches per beam. Solid line: no beam gaps; dashed line: one gap per beam of 13 missing bunches.

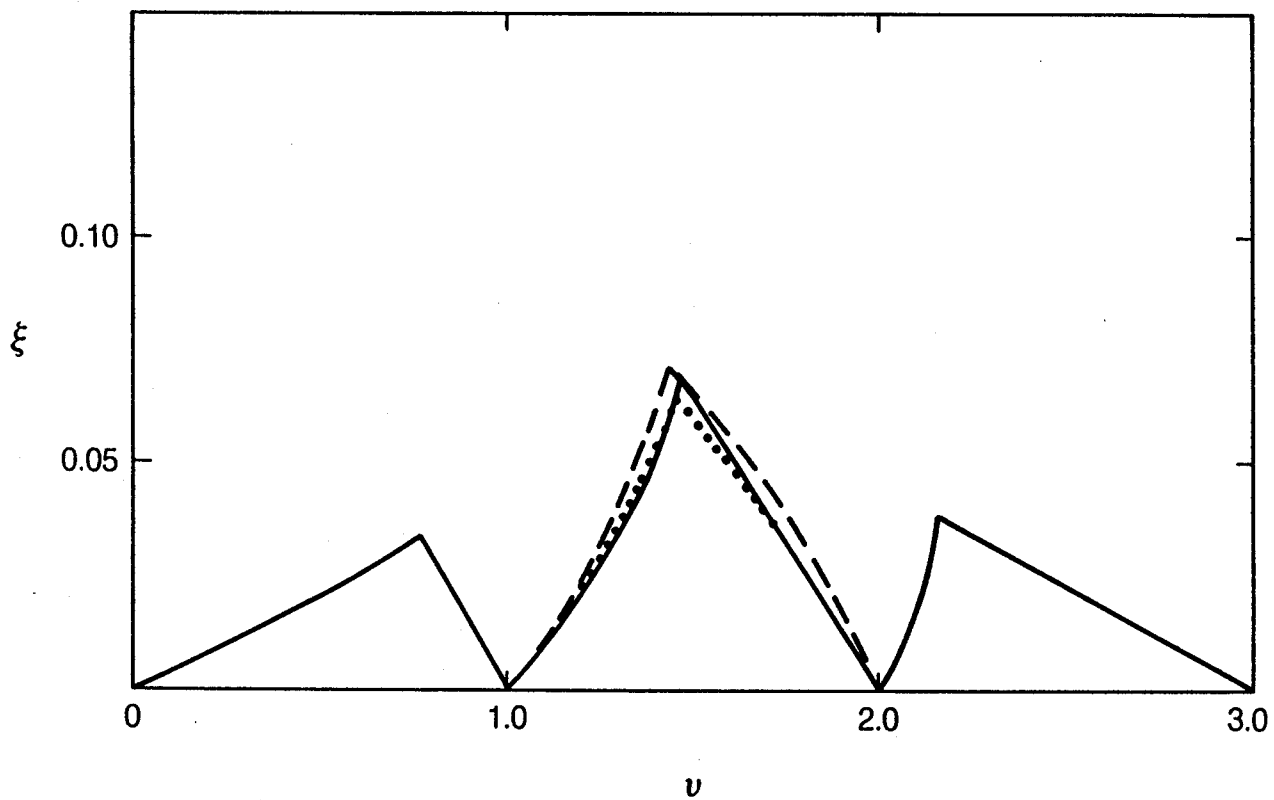


Fig. 9 Stability diagram for six identical IRs, distributed or clustered according to the (3,3) scheme. Solid line: distributed IRs and 198 bunches per beam; dashed line: clustered IRs and 102 bunches per beam; dotted line: clustered IRs and 198 bunches per beam.

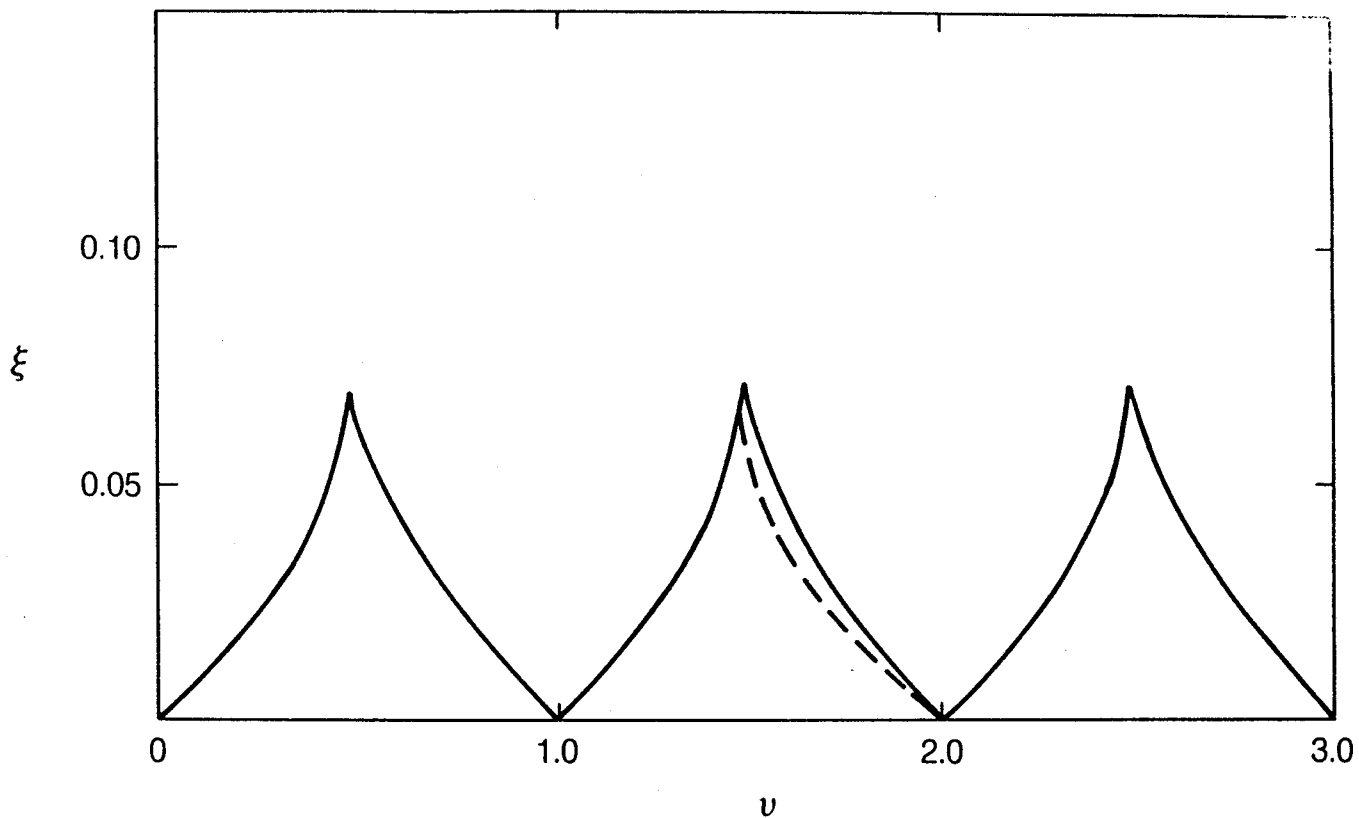


Fig. 10 Stability diagram for six identical clustered IRs, with the tune of the short arcs held fixed at 0.25. Solid line: 102 bunches per beam; dashed line: 198 bunches per beam.

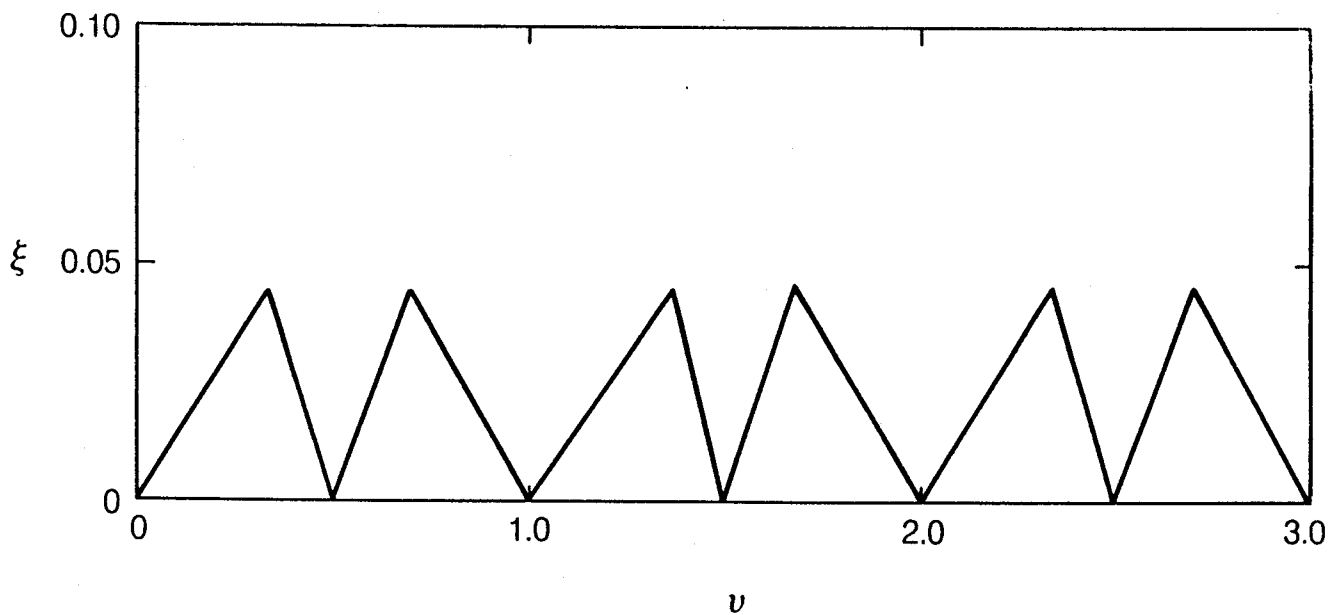


Fig. 11 Stability diagram similar to that of Fig. 10, except that the clustering scheme is (4,2) instead of (3,3). The tune of the short arcs is again held fixed at 0.25, and there are 102 bunches per beam.

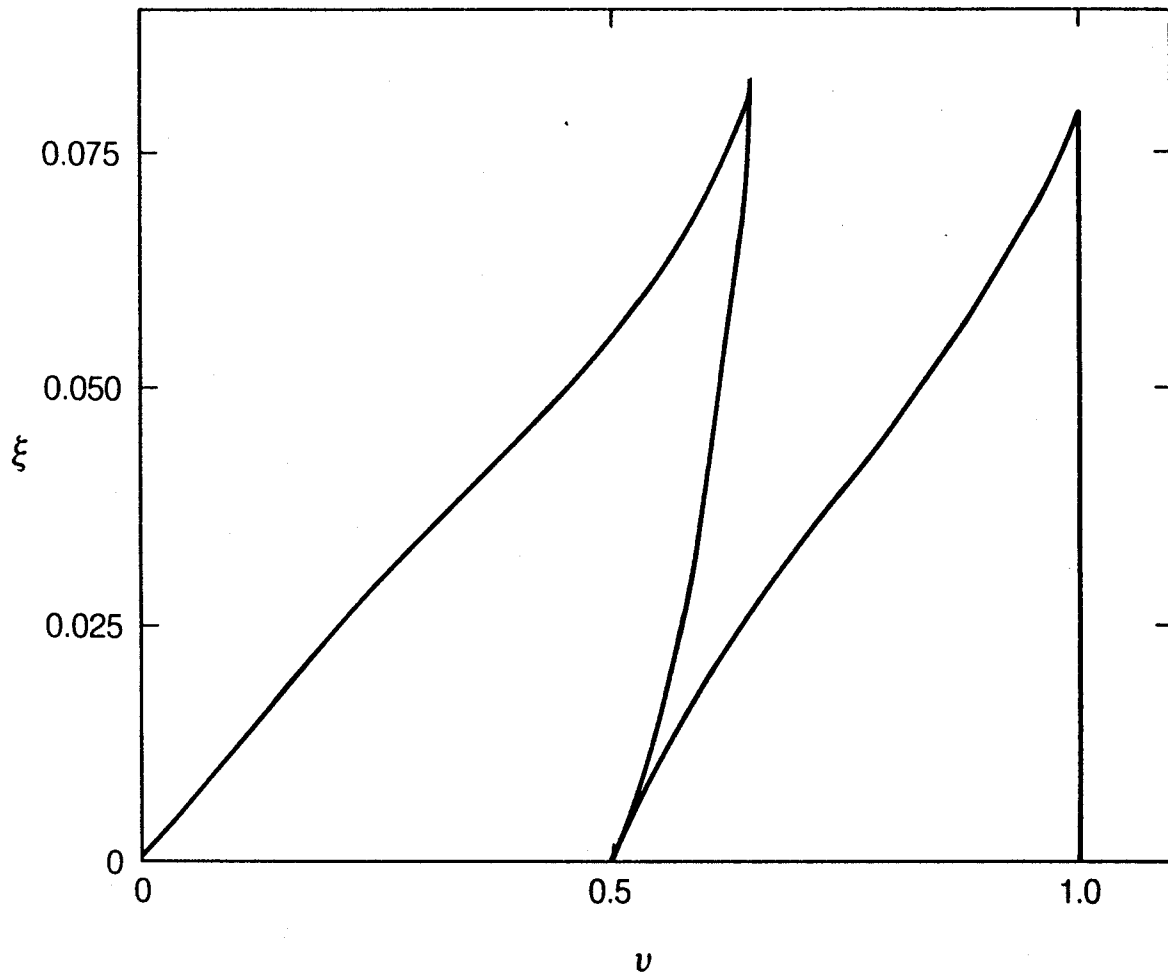


Fig. 12 Stability diagram for a lattice with four unequal clustered IRs, head-on collisions only and 26 bunches per beam; see text for details.

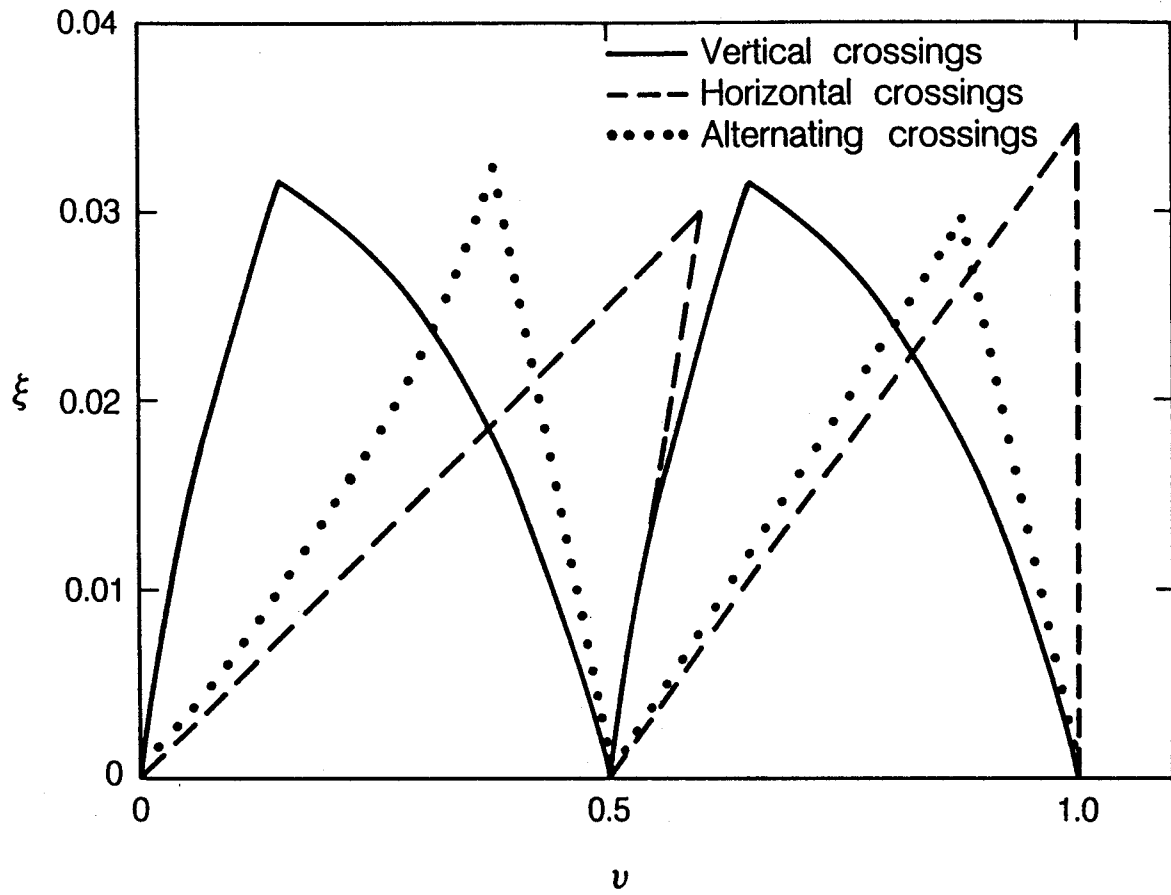


Fig. 13 Stability diagram for four unequal clustered IRs, similar to Fig. 12, except that long-range collisions are included (206 bunches per beam). The IRs have either purely vertical, purely horizontal, or alternating crossings.

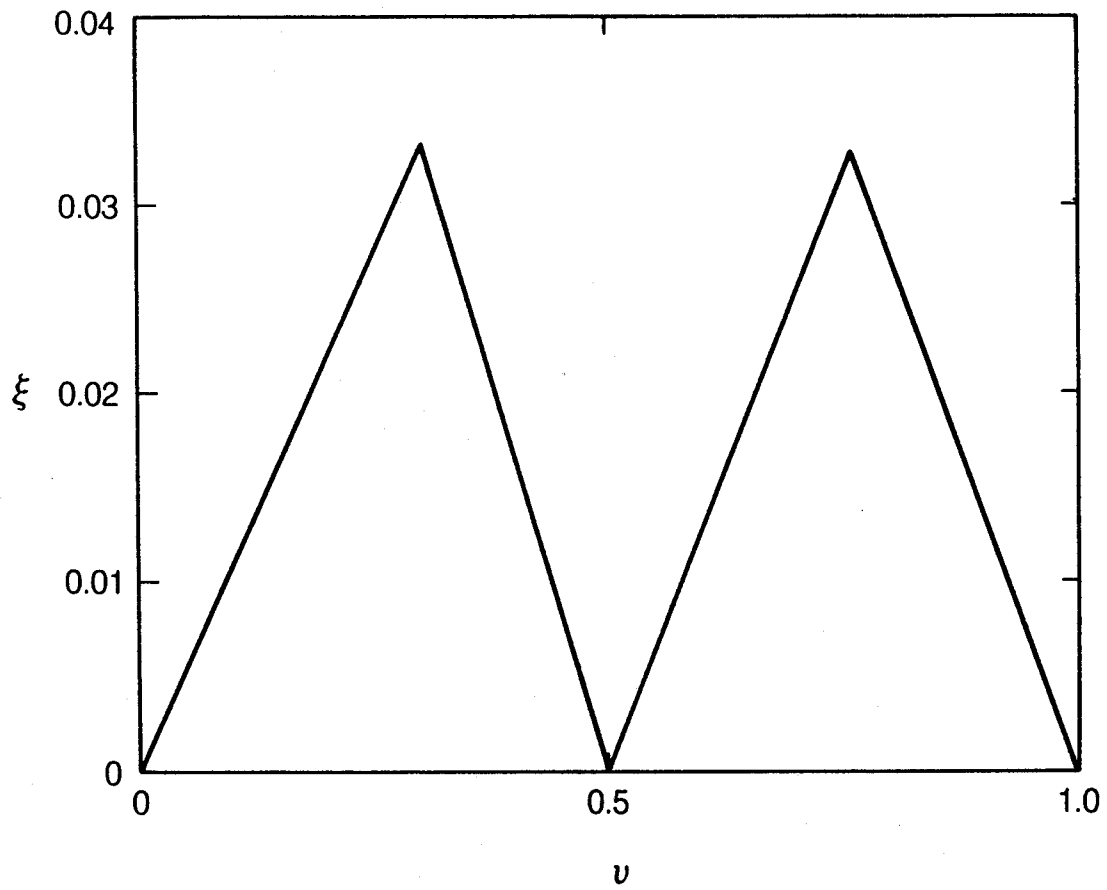


Fig. 14 Stability diagram for a nominal CDR lattice with six unequal IRs clustered according to the (4,2) scheme. The short arcs have fixed tune, and there are 332 bunches per beam.